Fixational eye movement: a negligible source of dynamic aberration

Pedro Mecê, Jessica Jarosz, Jean-Marc Conan, Cyril Petit, Kate Grieve, Michel Paques, Serge Meimon

Research Article | Vol. 9, No. 2 | 1 Feb 2018 | BIOMEDICAL OPTICS EXPRESS 717
Biomedical Optics EXPRESS

Fixational eye movement: a negligible source of dynamic aberration.

PEDRO MECÊ,[1,2] JESSICA JAROSZ,[1,2] JEAN-MARC CONAN,[1] CYRIL PETIT,[1] KATE GRIEVE,[3,4] MICHEL PAQUES,[3,4] AND SERGE MEIMON[1,*]

[1] *ONERA – the French Aerospace Lab, Châtillon, France*
[2] *Quantel Medical, Cournon d'Auvergne, France*
[3] *Clinical Investigation Center-CIC 1423 INSERM, Quinze-Vingts National Eye Hospital,Paris, France*
[4] *Institut de la Vision, Paris, France*
[*] *serge.meimon@onera.fr*

Abstract: To evaluate the contribution of fixational eye movements to dynamic aberration, 50 healthy eyes were examined with an original custom-built Shack-Hartmann aberrometer, running at a temporal frequency of 236Hz, with 22 lenslets across a 5mm pupil, synchronized with a 236Hz pupil tracker. A comparison of the dynamic behavior of the first 21 Zernike modes (starting from defocus) with and without digital pupil stabilization, on a 3.4s sequence between blinks, showed that the contribution of fixational eye movements to dynamic aberration is negligible. Therefore we highlighted the fact that a pupil tracker coupled to an Adaptive Optics Ophthalmoscope is not essential to achieve diffraction-limited resolution.

OCIS codes: (110.1080) Active or adaptive optics; (170.4460) Ophthalmic optics and devices; (170.4470) Ophthalmology; (010.7350) Wave-front sensing; (330.2210) Vision - eye movements.

References and links

1. P. Godara, A. M. Dubis, A. Roorda, J. L. Duncan, and J. Carroll, "Adaptive optics retinal imaging: emerging clinical applications," Optometry and Vision Science: Official Publication of the American Academy of Optometry **87**, 930–941 (2010).
2. A. Roorda and J. L. Duncan, "Adaptive optics ophthalmoscopy," Annual review of vision science **1**, 19–50 (2015).
3. J. Liang, D. R. Williams, and D. T. Miller, "Supernormal vision and high-resolution retinal imaging through adaptive optics," J. Opt. Soc. Am. A **14**, 2884–2892 (1997).
4. H. Hofer, P. Artal, B. Singer, J. Luis Aragón, and D. R. Williams, "Dynamics of the eye's wave aberration," J. Opt. Soc. Am. A **18**, 497–506 (2001).
5. J. Jarosz, P. Mecê, J. M. Conan, C. Petit, M. Paques, and S. Meimon, "High temporal resolution aberrometry in a 50-eye population and implications for adaptive optics error budget," Biomed. Opt. Express **8**, 2088–2105 (2017).
6. J. Arines, E. Pailos, P. Prado, and S. Bará, "The contribution of the fixational eye movements to the variability of the measured ocular aberration," Ophthalmic and Physiological Optics, **29**(3):281–287 (2009).
7. B. Sahin, B. Lamory, X. Levecq, F. Harms, and C. Dainty, "Adaptive optics with pupil tracking for high resolution retinal imaging," Biomed. Opt. Express **3**, 225–239 (2012).
8. K. Y. Li and G. Yoon, "Changes in aberrations and retinal image quality due to tear film dynamics," Opt. Express **14**, 12552–12559 (2006).
9. R. Montés-Micó, J. L. Alió, and W. N. Charman, "Dynamic changes in the tear film in dry eyes," Investigative Ophthalmology Visual Science, **46**(5), 1615 (2005).
10. S. Gruppetta, F. Lacombe, and P. Puget, "Study of the dynamic aberrations of the human tear film," Opt. Express **13**, 7631–7636 (2005).
11. C. Leahy, C. Leroux, C. Dainty, and L. Diaz-Santana, "Temporal dynamics and statistical characteristics of the microfluctuations of accommodation: Dependence on the mean accommodative effort," Opt. Express **18**, 2668-2681 (2010).
12. W. N. Charman and G. Heron, "Fluctuations in accommodation: a review," Ophthalmic and Physiological Optics **8**(2):153–164 (1988).
13. S. Martinez-Conde, S. L. Macknik, and D. H. Hubel, "The role of fixational eye movements in visual perception," Nature Reviews Neuroscience, **5**(3), 229–240 (2004).
14. I. P. V. Troxler, "Über das Verschwinden gegebener Gegenstände innerhalb unseres Gesichtskreises [On the disappearance of given objects from our visual field]," Ophthalmol. Bibl. **2**(2), 1–53 (1804).

#313630 https://doi.org/10.1364/BOE.9.000717
Journal © 2018 Received 16 Nov 2017; revised 20 Dec 2017; accepted 20 Dec 2017; published 22 Jan 2018

Biomedical Optics EXPRESS

15. S. Meimon, J. Jarosz, C. Petit, E. Gofas-Salas, K. Grieve, J. M. Conan, B. Emica, M. Paques, and K. Irsch, "Pupil motion analysis and tracking in ophthalmic systems equipped with wavefront sensing technology," Appl. Opt. **56**, D66–D71 (2017).
16. J. van de Kraats, T. Berendschot, and D. van Norren, "The pathways of light measured in fundus reflectometry," Vision research, **36**(15), 2229–2247 (1996).
17. D. Sliney, and M. Wolbarsht, *Safety with Lasers and Other Optical Sources* (Plenum Press, 1980).
18. D. Fanning, "Fit Ellipse," http://www.idlcoyote.com/programs/fit_ellipse.pro/ (2002).
19. S. T. Moore, T. Haslwanter, I. S. Curthoys, and S. T. Smith, "A geometric basis for measurement of three-dimensional eye position using image processing," Vision research **36**, 445–459 (1996).
20. R. J. Noll, "Zernike polynomials and atmospheric turbulence," J. Opt. Soc. Am. **66**, 207–211 (1976).
21. C. Kulcśar, H. F. Raynaud, and A. Garcia-Rissmann, "Eye-pupil displacement and prediction: effects on residual wavefront in adaptive optics retinal imaging," Biomed. Opt. Express **7**, 1051–1073 (2016).
22. P. C. L. Stephenson, "Recurrence relations for the Cartesian derivatives of the Zernike polynomials," J. Opt. Soc. Am. A **31**, 708–715 (2014).
23. T. O. Salmon, and C. van de Pol. "Normal-Eye Zernike Coefficients and Root-Mean-Square Wavefront Errors," Journal of Cataract Refractive Surgery **32**(12), 2064–2074 (2006).
24. J. Tabernero, P. Artal. "Lens Oscillations in the Human Eye. Implications for Post-Saccadic Suppression of Vision," PLoS ONE **9**(4), e95764 (2014).
25. A. Guirao, I. Cox, and D. R. Williams, "Effect of rotation and translation on the expected benefit of ideal contact lenses," in Vision Science and its Applications, OSA Technical Digest (Optical Society of America, 2000), paper PD2.
26. Q. Yang, J. Zhang, K. Nozato, K. Saito, D. R. Williams, A. Roorda, and E. A. Rossi, "Closed-loop optical stabilization and digital image registration in adaptive optics scanning light ophthalmoscopy," Biomed. Opt. Express **5**, 3174–3191 (2014).
27. A. Castro, L. Sawides, X. Qi, and S. A. Burns, "Adaptive optics retinal imaging with automatic detection of the pupil and its boundary in real time using Shack-Hartmann images," Appl. Opt. **56**, 6748–6754 (2017).

1. Introduction

Imaging the human retina at high-resolution has an important impact on early-stage retinal disease diagnosis and treatment as well as in monitoring the effects of new drugs and improving our understanding of the eye [1, 2]. Such high-resolution retinal images can be obtained using Adaptive Optics (AO) systems [3]. Most AO systems involve two main steps: measuring low and high order ocular aberrations with a wavefront sensor (WFS), usually a Shack-Hartman (SH); and compensating for them with a corrector device, often a deformable mirror (DM), in order to achieve diffraction-limited imaging.

The eye presents aberrations which are not static but fluctuate over time [4, 5]. Hence, the characterization and the understanding of these fluctuations are important in the design of AO systems, enable to correct them in real-time in a closed-loop configuration [5]. Several studies have been devoted to understanding the dynamics of ocular aberrations, as well as their origin. Fixational eye movements [6, 7], tear film dynamics [8–10] and micro-fluctuations of accommodation [11, 12] were identified as important sources of temporal variation of ocular aberration. However, the relative contribution of each of these elements remains unknown or incompletely known, especially concerning fixational eye movements, *i.e.*continuous and involuntary movements while the subject is looking at a fixation target. Fixational eye movements exhibit three main components [13]: 1) tremors, a wave-like motion of small amplitude ($\approx$ diameter of a cone in the fovea) but high frequency ($\approx$ 90 Hz); 2) drifts, slow movements (0.5deg/s) that carry the eye away from the fixation target (can move across dozens of photoreceptors) and 3) micro-saccades, fast ($\approx$ 20ms in duration), jerk-like movements (10-100deg/s) to correct from drifts and from Troxler fading [14].

Over a short range, these rotational ocular movements are seen from the point of view of AO system as synchronous retinal motion and pupil motion. The displacement of the pupil in front of the AO system induces an effective translation of the eye pupil and its aberrations over the eye pupil plane. Although aberrations in the pupil plane are dominated by static aberrations, the translation of this quasi-static aberration map over the wavefront sensor results in apparent wavefront variability (*i.e.*changes to the estimated wavefront coefficients). The relative importance

Biomedical Optics EXPRESS

of this source of aberration dynamics (compared to e.g. tear film dynamics) raises a controversial issue: on one hand Hofer *et al.* [4] concluded that the measured fluctuation in the eye's wave aberration is not due to pupil translation; on the other hand, Arines *et al.* [6] point out pupil translation as an important cause of apparent wavefront variability.

Subsequently, Sahin *et al.* [7] also claimed that eye movements constitute an important component of the ocular wavefront dynamics. They proposed an AO system with a static WFS, but coupled to a pupil tracking system. The DM compensates for aberrations by shifting the static wavefront measurement according to the pupil displacement measurement. They report a satisfactory aberration correction on average over time (i.e. a good correction of static aberrations), but the fluctuation of the wavefront error is minimally reduced, or not at all. Moreover, they mostly looked at low-frequency aberration fluctuation.

More generally, previous attempts to assess the contribution of fixational eye movements to aberration dynamics on healthy eyes [4, 6, 7] are limited in population (three eyes at most) and in aberrometer speed (25 Hz at most) and pupil tracker speed (83 Hz at most). In this paper, we make use of a previously published [5] high-temporal resolution characterization of ocular aberrations (sampling frequency of 236 Hz), synchronised with pupil displacement (at 236 Hz) on a population of 50 healthy eyes, in order to compare the dynamic behavior of the first 21 Zernike modes with and without digital pupil stabilization on a 3.4s sequence between blinks. We then conclude on the link between eye motion and wavefront variability.We also discuss the benefit of coupling a pupil tracker to AO-corrected ophthalmoscopes.

2. Methods

The high-resolution aberrometer used to characterize ocular dynamic aberrations was a custom-designed Shack-Hartmann (SH) wavefront sensor (WFS) coupled with a pupil camera for pupil motion tracking. Figure 1 shows a diagram of the full system. This system is composed of four units: 1) Injection unit, responsible for creating an artificial source on the retina for wavefront sensing; 2) eye unit, where the real or artificial eye is examined; 3) reference unit, allowing the calibration of the system and the acquisition of SH reference spots; 4) analysis unit, where the back-scattered light from the eye is collected by the WFS and the pupil camera.

A collimated infrared beam (833 nm superluminescent diode (SLED)(EXALOS) with 50-nm spectral bandwidth) is focused on the retina after passing through focus correction ophthalmic lenses adjusted according to the subject's refraction. Specular reflections from the cornea are filtered out by an annular pupil stop placed in a pupil plane. The use of infrared light increases the amount of light reflected by the retina [16], and is safer and more comfortable for the subjects. The WFS beacon itself is used as fixation target as it is at infinity and as part of its spectrum is in the visible range. The light backscattered from the retina is divided onto a pupil camera, composed of a CCD camera (up to 478 Hz, 1 pixel = 78 μm at the pupil) conjugate with the eye's pupil plane; and a SH WFS composed by a 31x33 microlens array (conjugate with the eye's pupil plane) with a 320 μm spacing and an sCMOS (Scientific Complementary Metal-oxide-Semiconductor) camera (Pco.Edge), with a 14x14 array of 196 pixels allocated per microlens, placed in the focal plane of the microlens array, which records the SH images with a sampling frequency of 236 Hz (i.e. grabbing 236 images per second). Both cameras image a 10-mm field in the pupil plane, but typically 22 microlenses are illuminated, which corresponds to a 7-mm diameter pupil allowing ± 1.5 mm pupil displacements, which is sufficient once the subject is stabilized by the chin and forehead rest (more details about the setup can be found in [5, 15]). Figure 2 shows the image map acquired from the SH WFS and pupil camera for a reference eye (*i.e.* an optical fiber source with pupil stop set at 7 mm).

A total of 50 healthy eyes, from 29 subjects, aged between 23-38 years old, of which 4 had undergone LASIK refractive surgery, were examined with the aberrometer. Subjects information such as age, spherical equivalent, cylindrical component J0 and J45 , pupil size and motion, and

Biomedical Optics EXPRESS

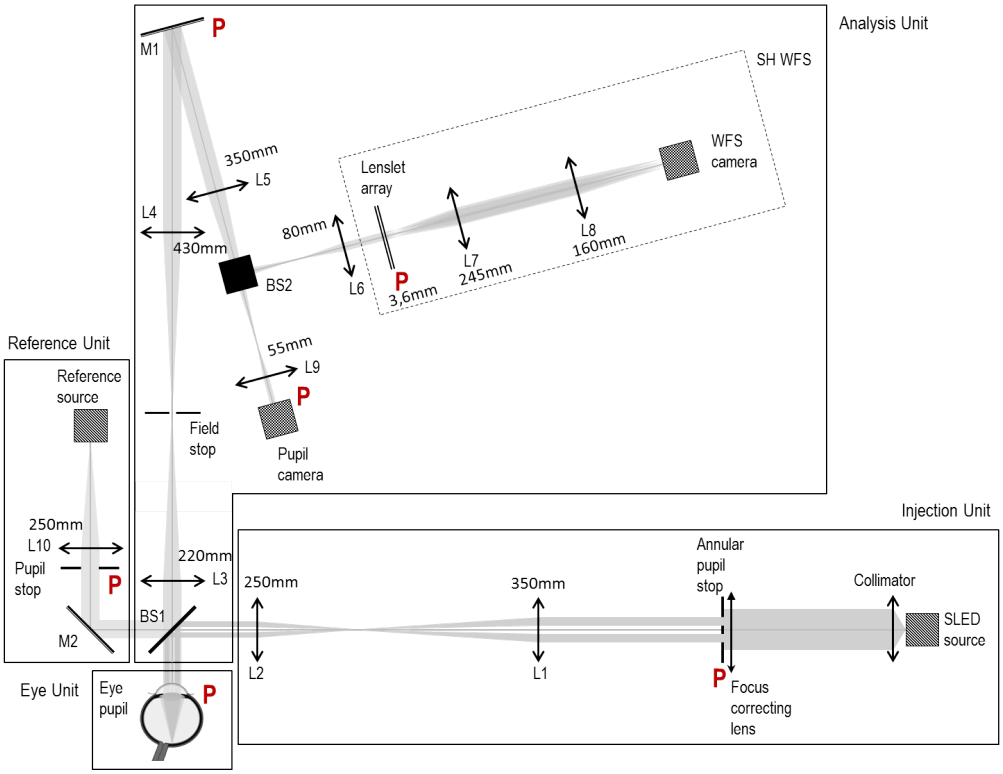

Fig. 1. Diagram of the experimental system (L: lens, BS: beam splitter, M: mirror, P: pupil plane). The four different units (injection, eye, analysis, reference) are outlined in the diagram.

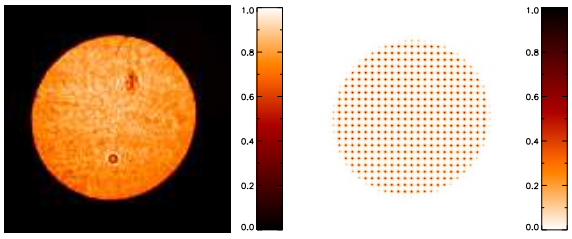

(a) Pupil Camera (b) Wavefront sensor

Fig. 2. Reference pupil intensity maps. (a) Pupil camera image. (b) SH WFS image.

Biomedical Optics EXPRESS

Zernike coefficients can be found in Data File 1 (supplementary data available for the reader). Prior to any measurements, each subject gave informed consent as part of the authorized clinical research protocol, which was approved by the local ethics committee and which adhered to the tenets of the Declaration of Helsinki. The optical power in the eye's pupil plane was set to be lower than 29 μW, approximately ten times less than the maximum permissible exposure for continuous viewing for this wavelength according to ANSI Z136.1 safety standard [17], and background and reference images were acquired on the WFS.

Measurements were performed without any pupil dilation or drops, as we were interested in characterizing the dynamic aberrations without the interference of any external factors. Visible light was kept to a minimum during the examination, thus leading to the largest possible pupils without dilation. Subjects were asked to blink just before the acquisition started and to sit still and stare at the point source throughout the acquisition period. The acquisition lasted 20 seconds per eye. The raw data consisted of 50 series of synchronized 20-second-long WFS camera and pupil camera sequences, both at 236 Hz. Then for all 50 eyes, we extracted a continuous 3.4 s time sequence (i.e., 808 frames) in between blinks.

For each 3.4-second-long sequence from the pupil camera, pupil motion and pupil size were computed on binarized images and pupil tracking was performed based on an ellipse fitting algorithm [18], which compensates for geometric distortions from image projection [19]. Pupil position precision was estimated to 2 μm RMS. Details of the data processing for pupil tracking can be found in [15].

In order to analyze the contribution of eye motion (especially pupil translation) on the dynamics of ocular aberrations, we defined two different analysis pupils (P_a), illustrated in Fig. 3:

Without digital pupil stabilization: In this case, the analysis pupil (P_a) is fixed on the WFS while the eye pupil (P_{eye}) moves.

With digital pupil stabilization: In this case, the analysis pupil (P_a) is fixed at the center of the eye pupil (P_{eye}) for each time t and therefore, it moves on the WFS, allowing us to show how the aberration dynamics evolve independently of pupil translation.

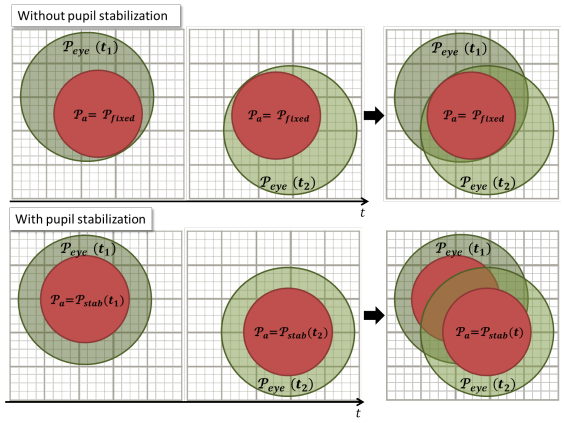

Fig. 3. Definition of a 5-mm analysis pupil (P_a) in order to quantify dynamic aberration evolution with and without digital pupil stabilization over time. Without pupil stabilization: P_a is fixed on the WFS while the eye pupil (P_{eye}) moves. With pupil stabilization: P_a is fixed at the center of the eye pupil (P_{eye}) for each time t and therefore, it moves on the WFS.

For each time-point of each sequence, we built an analytic WFS model M_{WFS}, which depends on the eye and on the analysis pupil (with or without stabilization), linking the Zernike coefficient

Biomedical Optics EXPRESS

at a time t ($a_i(t, eye)$) to the slopes of the subapertures at the same time ($S(t, eye)$):

$$S(t, eye) = M_{WFS}(eye, P_a) \cdot a_i(t, eye) \quad (1)$$

By taking the pseudo inverse $M_{WFS}(eye, P_a)^{\dagger}$, Zernike coefficients can be reconstructed [5] for both analysis pupils (with or without stabilization):

$$a_i(t, eye) = M_{WFS}(eye, P_a)^{\dagger} \cdot S(t, eye) \quad (2)$$

For each 3.4-second-long sequence from the SH WFS, the Zernike decomposition (from 2^{nd} to 5^{th} order) of the wave aberration was computed with and without stabilization. In accordance with convention [20], we will refer to aberration modes with a radial order greater than or equal to 3 as high-order aberration (HOA). Static wavefront error ($\sqrt{\sum_{i=4}^{21} \bar{a_i}^2}$) was used to quantify the level of static aberrations.

3. Results

Figure 4 shows temporal series of horizontal (black line) and vertical (magenta line) pupil translation, and temporal series of the first seven Zernike coefficients, starting from defocus (a_4) for three different eyes, without pupil stabilization. Figures 4(a), (d) and (g) illustrate eye 13, a LASIK case, which presents a high wavefront error (WFE), a significant high-order aberration (HOA) WFE and a poor fixation in relation to the population studied. Figures 4(b), (e) and (h) show eye 16, the poorest fixation case, which presents a typical WFE. Finally, Figs.4(c), (f) and (i) present eye 31, a typical case of our population, *i.e.*both fixation eye movements and WFE do not exceed the average ± standard deviation of 50-eyes population studied. Information on eyes 13, 16 and 31, as well as the general population, can be found in table 1.

Table 1. Population (mean ± standard deviation) and eyes 13,16,31 (mean values) information concerning age, horizontal (H) and vertical (V) pupil translation standard deviation, wavefront error, high-order wavefront error and the specificity of each case compared to the studied population as a whole.

Eyes	Population	Eye 13	Eye 16	Eye 31
AGE (yo)	30±7	27	35	25
Fixational eye movement Standard Deviation (μm)	H:48±23, V: 30±14	H:110.4, V: 38.3	H:116.6, V: 19.1	H:28.9, V: 31
Static Wavefront Error (WFE) (μm)	0.59 ± 0.31	1.25	0.31	0.34
High-order aberration WFE (μm)	0.21 ± 0.10	0.69	0.20	0.19
Specificity	–	Lasik case and poor fixation	Poor fixation	Typical case

Dashed lines highlight fast horizontal micro-saccade occurrences for eyes 13 and 31 and a large amplitude horizontal drift occurrence for eye 16. For all three eyes, we can identify horizontal tremors. Eye 13 presents a major correlation between pupil horizontal shift, in particular fast and large amplitude translation (micro-saccades) and Zernike coefficients a_5 (oblique astigmatism) and a_8 (horizontal coma), with a linear Pearson correlation coefficient $r_5 = 0.91$ and $r_8 = 0.77$ respectively. Eye 16 presents a major correlation between pupil horizontal shift, in particular slow and large amplitude translation (drifts) and the same Zernike coefficients

Biomedical Optics EXPRESS

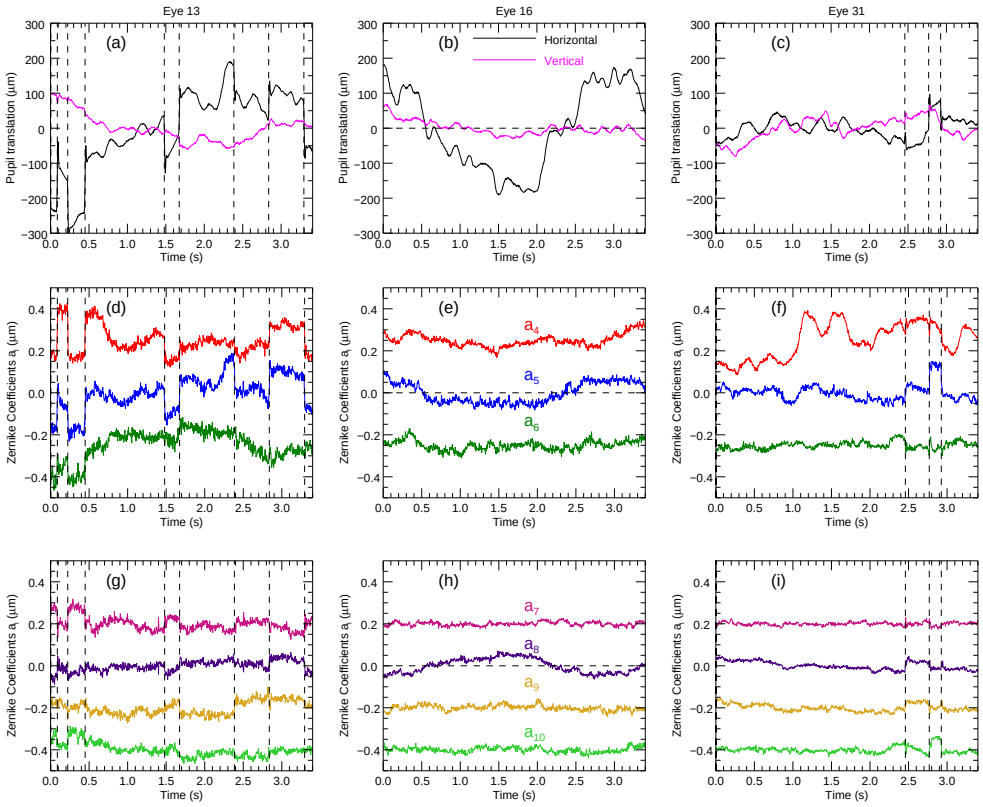

Fig. 4. Illustration of the correlation between eye movements and dynamic aberrations.(a), (b) and (c) : horizontal (black line) and vertical (magenta line) pupil translation of eyes 13, 16 and 31 respectively. (d), (e) and (f): second order Zernike coefficients time series without pupil stabilization of eyes 13, 16 and 31 respectively. (g), (h) and (i): third order Zernike coefficients time series without pupil stabilization of eyes 13, 16 and 31 respectively. Modes are attributed different colors and are specified in (e) and (h). The plots have been vertically shifted for clarity. As a consequence, mean values do not represent static aberrations. Vertical dashed lines highlight fast and large horizontal micro-saccade occurrences for eyes 13 and 31. Horizontal dashed lines indicate slow and large amplitude horizontal drift occurrence for eye 16.

Biomedical Optics EXPRESS

a_5 (oblique astigmatism) and a_8 (horizontal coma), with a correlation coefficient $r_5 = 0.93$ and $r_8 = 0.94$ respectively. Finally, eye 31 presents a minor correlation between pupil shift and Zernike coefficients (correlation coefficient lower than 0.3). On the other hand, eye 31 presents a significant correlation between micro-saccade occurrences and Zernike coefficient a_5. Although horizontal tremors are present in all cases, no correlation was found between them and dynamic aberration.

A strong correlation between motion and aberration does not necessarily mean *causality*, *i.e.*that aberration originates from pupil displacement at WFS, a third factor may be at the origin of both phenomena. In order to test the causality of pupil translation for dynamic aberration, we quantified the fluctuation over time of each Zernike mode across a 5-mm diameter pupil, with and without pupil stabilization, over our population.

First, we calculated the temporal standard deviation of the first 21 Zernike coefficients $\sigma_t(a_i(t, eye))$ (starting from defocus), with and without pupil stabilization. To study the general trend over the population we evaluated the average (± standard deviation) of $\sigma_t(a_i(t, eye))$ over the population. The results are displayed in Fig. 5. We see that two modes are slightly impacted by pupil translation compensation: oblique astigmatism (a_5), which presents an average value 12% lower when the pupil is digitally stabilized and a standard deviation (over the population) 35% lower; and horizontal coma (a_8), which presents an average value 16% lower and a standard deviation (over the population) 23% lower.

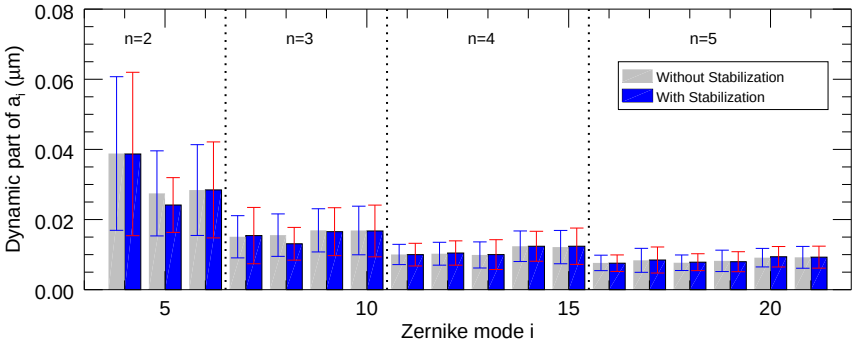

Fig. 5. Distribution of the dynamic aberration over the population with and without pupil stabilization. Zernike coefficients from the 2^{nd} to the 5^{th} order over the population across a 5-mm diameter pupil. Silver and blue bars indicate average of $\sigma_t(a_i(t, eye))$ over the population, with and without pupil stabilization respectively. Blue and red error bars indicate plus and minus one standard deviation of $\sigma_t(a_i(t, eye))$ over the population, with and without pupil stabilization respectively.

4. Discussion

Dynamic aberrations, without pupil stabilization, can be decomposed into three main components, low, medium and high-frequency [5]. By considering a 3.4s long analysis sequence, for each eye of our 50 eye population, we were able to study medium and high-frequency fluctuations of each Zernike coefficient (evolutions at frequencies below 0.3 Hz are seen as static). These fluctuations could be due to tear film dynamics, eye motion (pupil translation) or lens fluctuation. By digitally stabilizing the pupil, we were able to study the impact of eye motion over medium and high-frequency fluctuation of the wavefront. Figure 4 illustrates a visible correlation between horizontal pupil translation and some Zernike coefficient fluctuations such as oblique astigmatism (a_5) and horizontal coma (a_8). The observed correlation is mainly highlighted for two fixational

Biomedical Optics EXPRESS

eye movements: fast (10-20ms duration) horizontal micro-saccades and large amplitude horizontal drifts. Tremor movements were weakly correlated to the fluctuation level of aberrations.

Thus, we can assume two possible scenarios regarding wavefront variation:

"moving aberration" assumption [21], where the dynamic aberrations are mainly due to the displacement of a static phase on the WFS. In this case, fluctuation of Zernike coefficients with time would be *significantly decreased* by stabilizing the pupil;

"turmoil aberration" assumption, where the contribution of eye motion to dynamic aberrations is negligible. In this case, fluctuation of Zernike coefficients with time will be *unchanged* after stabilizing the pupil.

As shown in figure 5, the "turmoil aberration" model is correct. Let us examine how this applies to each Zernike mode:

- as regards a_5, a 12% decrease of the average $\sigma_t(a_i(t, eye))$ (over the population) is observed when stabilizing the pupil (cf. Fig. 5). However, a more precise analysis shows that this decrease actually occurs only for three specific eyes, two being Lasik cases (eyes 13 and 14, belonging to the same subject, with major high-order aberration WFE and poor fixation) and one (eye 16) with medium static aberrations and the poorest fixation of the population. In other words, except for poor fixators with significant static aberrations, the "turmoil aberration" model holds;

- as regards a_8, a 16% decrease of the average $\sigma_t(a_i(t, eye))$ (over the population) is observed when stabilizing the pupil (cf. Fig. 5). Unlike for a_5, this limited but significant decrease is shared by most of the eyes in our population, suggesting an actual "moving aberration" component in a_8 dynamics. Indeed, we identified that a horizontal motion, in conjunction with the presence of spherical aberration, produces a fluctuation of a_8 (see Fig. 6). It turns out that average static spherical aberration measured on our population is slightly positive ($a_{11}^{stat} = 0.06\mu m \pm 0.05\mu m$), which was also observed by Salmon *et al.* [23]. We then conclude that a moderate part of a_8 dynamics is due to pupil motion;

- as regards *any other mode*, the fluctuation of Zernike coefficients with time is not decreased with pupil stabilization.

This, however, does not explain the severe changes in aberration distribution occurring at the exact same time as saccades. Although this specific topic is outside the scope of the present paper, such correlation could be explained by crystalline lens shape change after a shift in the line of sight, or lens wobbling, which have been shown to have a significant impact on high-order aberrations [12, 24]. One limitation of the present study is that torsional eye rotations (inducing a pupil rotation) [25] were not taken into account in this study. However, a 3.4s time series should be sufficiently short to avoid significant torsional eye rotations [26]. Moreover, a monochromatic and point source fixation target is not ideal. Nonetheless the use of a "poor" fixation target, and the consequent possible increase in fixational eye movements, served to demonstrate the fact that fixational eye movement is a negligible source of dynamic aberration.

Finally, individual temporal series of the first Zernike coefficients (starting from defocus) with and without pupil digital stabilization are available upon request to the last author. Even if in some cases (such as poor fixators and eyes presenting a high static level of high order aberration WFE) a pupil stabilization may be beneficial, the corresponding reduction of the aberration fluctuation standard deviation is minor (1% in average, 30% at most for eye 16). Therefore pupil tracking in an Adaptive Optics Ophthalmoscope is not essential to achieve diffraction-limited resolution, but it can help to automatically detect the pupil and its boundary and avoiding missing spots in the SH WFS [27]. A far more effective way to correct dynamic aberration would be to increase sampling frequency up to 40 Hz with a loop gain of 0.5 [5].

Biomedical Optics EXPRESS

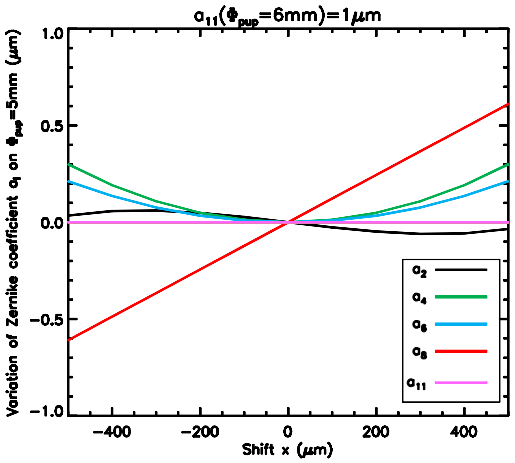

Fig. 6. Effect of static spherical aberration and horizontal displacement on the other modes, derived from the linear expansion published in [20, 22].

5. Conclusion

Using previously published data [5] of high-temporal resolution characterization of ocular aberrations (at a sampling frequency of 236Hz) synchronised with pupil displacement (at 236 Hz) on a population of 50 healthy eyes, we presented a comparison of the dynamic behavior of the first 21 Zernike modes, with and without digital pupil stabilization, on a 3.4s sequence between blinks. First, our results showed a major correlation between dynamic aberration and two fixational eye movements: fast horizontal micro-saccades and large amplitude horizontal drifts. In order to study the causality between both factors, we calculated the standard deviation over time of the first 21 Zernike modes with and without pupil stabilization and we compared them. In a "turmoil aberration" assumption, where the contribution of the eye motion to dynamic aberrations is negligible, the fluctuation of Zernike coefficient with time will be unchanged after stabilizing the pupil. We showed that for mode a_5 (oblique astigmatism), except for poor fixators with significant static aberrations, the "turmoil assumption" holds. In the case of a_8 (horizontal coma), a moderate part of its dynamic is due to pupil motion. Finally, for any other mode, the fluctuation of the Zernike coefficient with time is not decreased with pupil stabilization, showing that the contribution of fixational eye movement to dynamic aberration is negligible. Therefore we highlighted the fact that a pupil tracker coupled to an Adaptive Optics Ophthalmoscope is not essential to achieve diffraction-limited resolution in healthy undilated eyes.

Funding

Agence Nationale de la Recherche under grants CLOVIS3D (grant number ANR-14-CE17-0011) and RHU LIGHT4DEAF (grant number ANR-15-RHUS-0001).

Disclosures

PM: Quantel Medical (E)